Journal of ELECTRICAL ENGINEERING, VOL. 57, NO. 6, 2006, 354–359

FERMI LEVEL ANALYSIS OF GROUP III NITRIDE SEMICONDUCTOR DEVICE STRUCTURES BY AUGER PEAK POSITION MEASUREMENTS

Gernot Ecke [*] — **Merten Niebelschütz** [*] — **Rastislav Kosiba** [*] — **Uwe Rossow** [**] — **Volker Cimalla** [*] — **Jozef Liday** [***] — **Peter Vogrinčič** [***] — **Jörg Pezoldt** [*] — **Vadim Lebedev** [*] — **Oliver Ambacher** [*]

The peak position of characteristic Auger transitions depends on the position of the Fermi level of the sample electrons. Thus, Auger electron spectroscopy can be applied for detection of semiconductor conduction type with a high lateral resolution typical for Auger electron spectroscopy mapping. Moreover, the peak position can be evaluated, even if the semiconductor surface is cleaned by sputtering. In this work, the Auger peak position measurements have been applied to GaN p-n-junctions as in cross section geometry as well as in Auger depth profiles. The method has also successfully been applied to n- and p- type doped AlGaN, and to Mg doped InN samples. It was observed that the differences in Auger peak positions from n- to p-type GaN and AlGaN differ from the theoretical prediction due to the impact of surface charges and additional band bending effects induced by the sputtering process.

K e y w o r d s: group III nitrides, sputter depth profiling, Auger Electron Spectroscopy, Auger peak position, Fermi level

1 INTRODUCTION

Direct wide band gap semiconductors such as group III-nitrides are the basis of modern optoelectronic devices, *eg* laser, light emitting diodes and sensors. Analyses of those devices need nanoscale spatial and depth resolutions. However, only a few analytical methods have the requested resolution capability. One of them is Auger electron spectroscopy (AES). Modern Auger spectrometers have a lateral resolution down to 10 nm, while the depth resolution of sputter profiles is in the range of a few nanometers depending on sputter conditions and material properties. Although the Auger electron spectroscopy is usually not able to detect dopants in the concentration range far below $10^{20}\mathrm{cm}^{-3}$, the position of the Auger peaks are sensitive to the position of the Fermi level and therefore to the doping [1–3]. Thus, little amounts of electrically active dopants can be detected even if their concentration is orders of magnitude lower than the detection limit of the analytical method. This capability could be shown for silicon in the past, where p-and n-type material resulted in Auger electron peak shifts of about 0.6 eV [1, 2]. This effect is even stronger for wide band gap semiconductors. In the case of silicon carbide the Auger peak position analysis could distinguish between n- and p-type as well as between 3C and 6H material [3]. Recent works have been published for the detection of strain in GaN structures by Auger peak position analysis [4]. In group III- nitride technology p-type doping by Mg has proved to be problematical. Auger peak position analysis gives an easily applicable tool for testing the p-type doping of structured GaN layers. The peak position analysis in Auger electron spectroscopy is working even if the material is ion beam sputtered. Ion beam induced surface charging and other charging effects result in additional Auger peak shifts. The physical background of this method is discussed and successful applications of this method on optoelectronic device structures such as vertical pn-junctions as well as on lateral polarity structures of gallium nitride are shown.

2 EXPERIMENTAL

The samples, which have been measured by Auger electron spectroscopy, were grown by PIMBE (p- and n-GaN, lateral polarity) and MOCVD (pn-junction, p-GaN). If necessary, the layer thickness and the behaviours of the electrical measurements are referred in the text. Electrical measurements confirmed the conduction type of the layers and the typical band gap of 3.45 eV for GaN.

The Auger electron spectroscopic measurements have been carried out by a Thermo Microlab 350 (Ilmenau) and a Varian Auger Spectrometer (Bratislava), respectively. Measurement parameters for the Microlab 350 were: electron beam of approximately 1 nA, spot diameter of 15 nm, measurement of the kinetic energies with a

[*] Technical University Ilmenau, Center for Micro- and Nanotechnologies, P.O. Box 100565, D-98684 Ilmenau, Germany; E-mail: gernot.ecke@tu-ilmenau.de; [**] Technical University Braunschweig, Institute for Technical Physics, Mendelssohnstr. 2, D-38106 Braunschweig, Germany; [***] Slovak University of Technology, Institute for Microelectronics, Ilkovičova 3, 81219 Bratislava, Slovakia, E-mail: jozef.liday@stuba.sk

ISSN 1335-3632

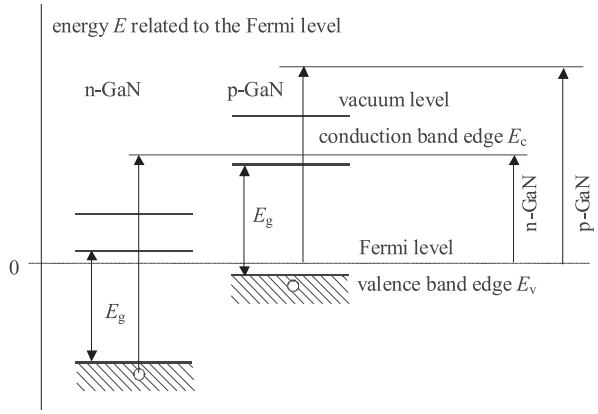

Fig. 1. Schematic energy behaviour of an Auger electron emission of p- and n-doped GaN

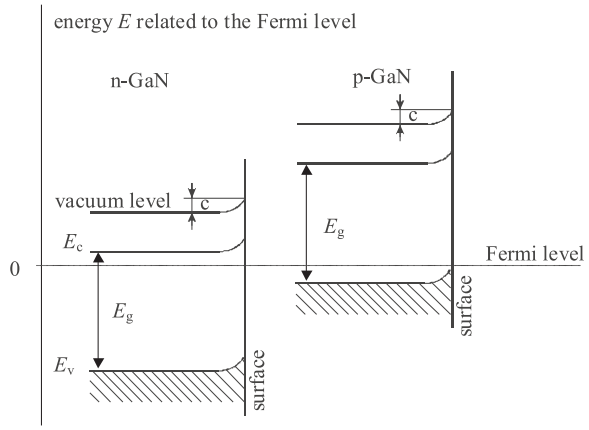

Fig. 2. Energy scheme of sputtered p- and n-doped GaN with sputtering induced surface charge leading to a band bending of c

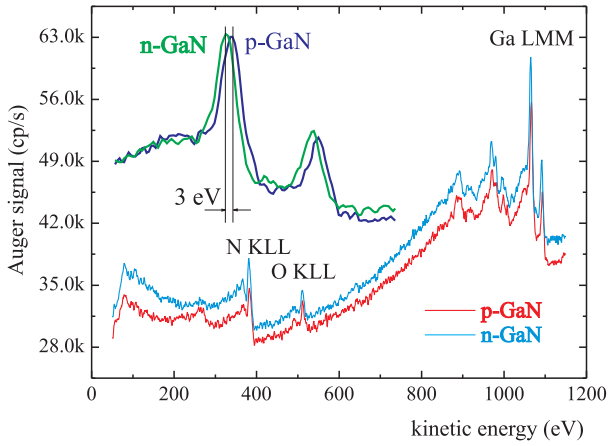

Fig. 3. Auger spectrum survey of n- and p-type GaN heteroepitaxial layers, the insert shows the Ga LMM peaks

hemispherical analyser with constant retard ratio of 4 in direct mode; a primary electron energy of 5 kV under 60° irradiation with respect to the surface normal. Sputtering war carried out by 1 keV Ar scanned ion beam ($1\,\mathrm{mm}^2$) with an angle of 70° with respect to the surface normal. Measurement parameters for the Varian Auger analysis were: 3 keV primary electron beam scanned over an area $300 \times 300\,\mu\mathrm{m}^2$, normal incidence, energy resolution of the CMA $\Delta E/E = 0.3\,\%$. The samples were sputtered by a scanned Ar ion beam (0.5, 1, and 4 keV) striking the surface over an area of $300 \times 5000\,\mu\mathrm{m}^2$ at 80° with respect to the normal. For the peak position measurements the Ga MVV, the N KLL and the Ga LMM Auger transitions have been measured. The O KLL and C KLL Auger peaks have been checked to ensure perfect sputter cleaning of the surface.

3 BASIC CONSIDERATIONS

The energy of an Auger electron generated in a solid is defined by equation (1) according to [3]:

$$E_{\mathrm{kin}}(UVW) = E(U) - E(V) - E(W) - F(x) + R^{ia} + R^{ea} \quad (1)$$

with $E_{\mathrm{kin}}(UVW)$ — the kinetic energy of the Auger electron, $E(U)$, $E(V)$ and $E(W)$ — the shell energies of the solid according to the sample Fermi level, $F(x)$ — the interaction energy of the two positively charged final states, R^{ia} — the intraatomic relaxation energy and R^{ea} — the extraatomic relaxation energy.

All the energy levels of the shells and subshells are related to the Fermi level of the material. If we measure the kinetic energy of an Auger electron with respect to the Fermi level and if we assume the interaction energy $F(x)$, the intraatomic relaxation R^{ia} and the extraatomic relaxation R^{ea} energies to be equal in p- and n-GaN, we can see, that the difference of the Auger energies depends on the difference of the Fermi level position in the p- and n-material. Assuming a shift of the work function of δ from p- to n-type GaN, we can calculate the difference of the Auger electron energy ΔE of all Auger peaks in the spectra from n- to p-GaN (equation (2)):

$$\Delta E = E_{\mathrm{kin}}^{p-GaN}(UVW) - E_{kin}^{n-GaN}(UVW) = E(U) - E(V) - F(x) + R^{ia} + R^{ea} - \left[(E(U)+\delta) - (E(V)+\delta) - (E(W)+\delta) - F(x) + R^{ia} + R^{ea}\right] = \delta\,. \quad (2)$$

The energy behaviour of an Auger electron emission of p- and n-doped GaN according to equation (2) is demonstrated schematically in Fig. 1.

However, in praxis all surfaces are contaminated by air or by thin adsorbate layers from the technological process or the surface is oxidized. The contaminations as well as charged surface states lead to a band bending, so that the energy scheme and Auger electron behaviour as shown in Fig. 1 is not valid at a real surfaces. The most frequently applied method for surface cleaning in surface analysis is ion beam sputtering, mostly by noble gas ions. Nevertheless, sputtering not only removes material from the surface, but there are a lot of additional effects like atomic mixing, preferential sputtering or damaging the surface crystallinity [5]. Ion beam induced surface damage heavily depends on the sputtering conditions such as beam energy, angle of incidence and ion species as well as on

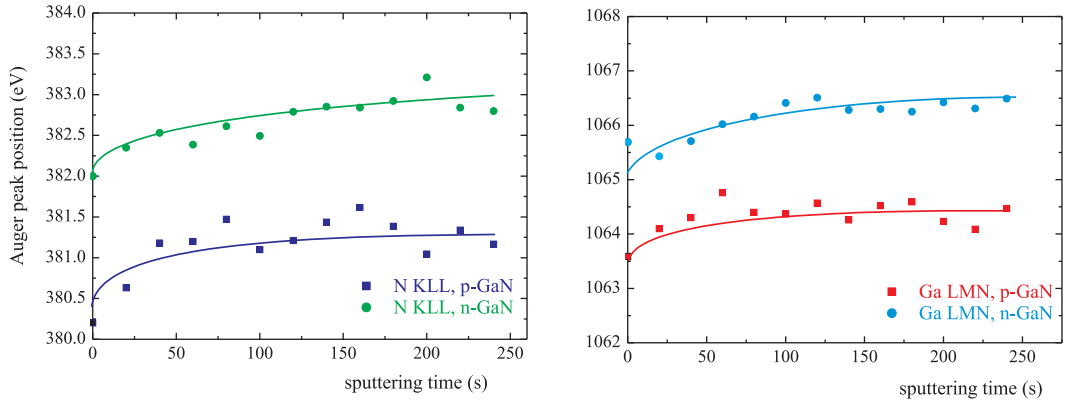

Fig. 4. Auger peak position development of N KLL and Ga LMM Auger peaks during sputter etching for p- and n-doped GaN

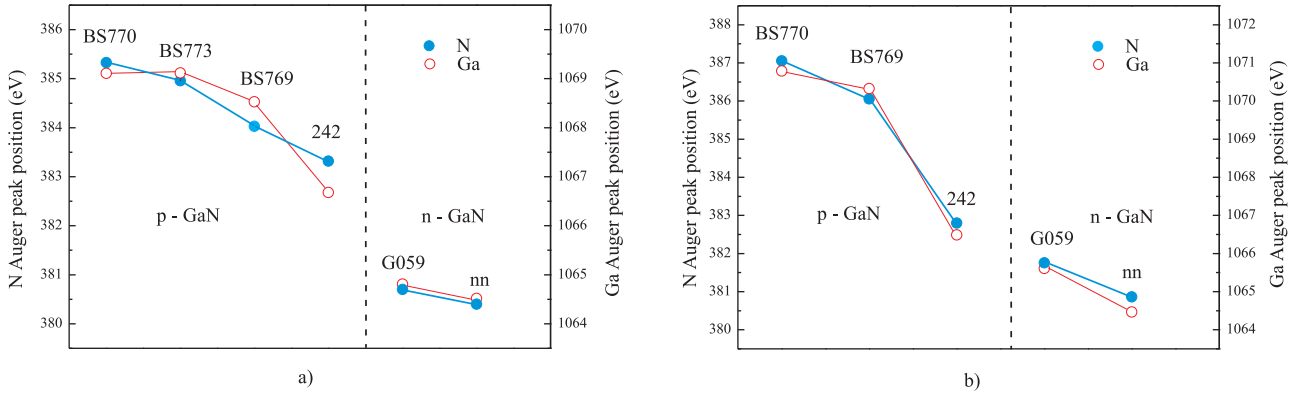

Fig. 5. Auger peak positions for different samples of p- and n-doped GaN a) as loaded and b) sputter cleaned for the N KLL and Ga LMM Auger peak

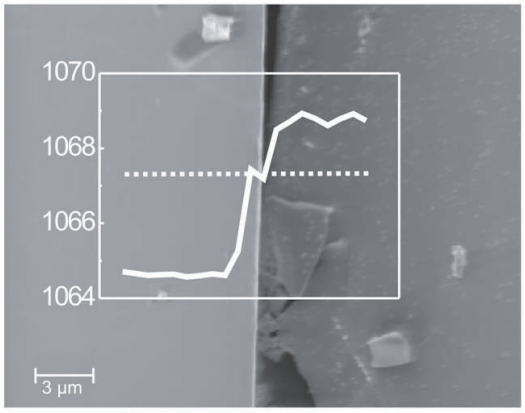

Fig. 6. Scanning electron micrograph of the lateral pn structure, the position of the scanned line and the Auger peak position of the Ga LMM Auger peak

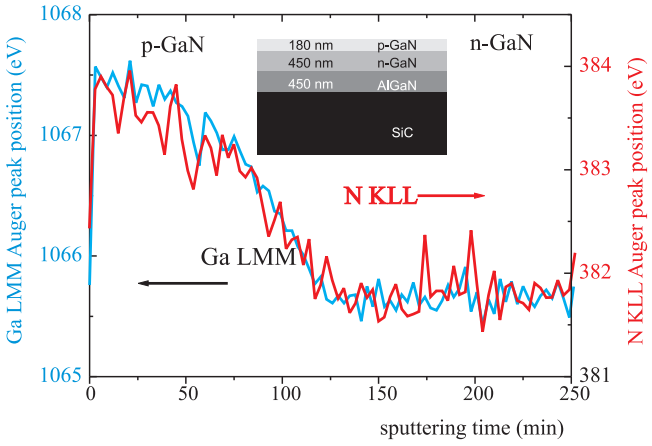

Fig. 7. Auger depth profile of the vertical pn-junction; results for the Ga LMM and N KLL Auger peak

the target composition and crystallinity [5]. But the surface damage and therefore the creation of additional surface charge should not depend on the doping of a sample, if the other properties do not differ. Applying the same sputtering conditions to n- and p-GaN and thus, if we assume equal ion beam induced surface charges and band bending for both, n- and p- type GaN as shown in Fig. 2, the difference of the Auger peak energy as calculated by equation (2) should be approximately the same, even for sputtered material. Consequently, it should be possible to detect differences between n- and p-doped GaN layers, even if the surface is sputter cleaned. In order to produce a minimum of sputtering induced surface charge and thus, a minimum sputtering induced band bending and peak shifts, the sputtering conditions should be properly chosen for 'soft' sputtering, *ie* low ion energy, gracing incidence and, if possible heavy ion species. Generally we know, that Auger peak shifts are caused by (i) differ-

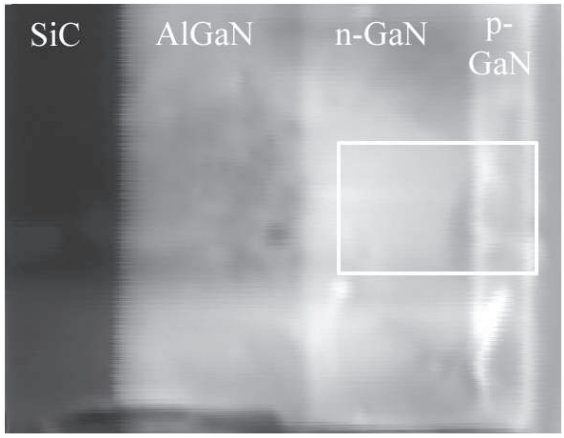

Fig. 8. Cross section of the vertical pn-junction sandwich sample with the area selected for Auger mapping

ences in the position of the Fermi level in the semiconductor bulk material and (ii) band bending according to sputtering and surface charges. There are some additional factors causing band bending and Auger peak shift such as (iii) the internal electrostatic field of the pyroelectric material and [6] (iv) removal of adsorbate layers and surface oxide and (v) changing of the surface potential due to the voltage drop caused by the electron current in case of high resistivity layers. The latter can be avoided using low current and its influence can be tested by measuring the Auger peaks position by different beam currents. If the peak position does not depend on the beam current, this influence can be neglected.

4 RESULTS AND DISCUSSION

4.1 Galliumnitride

uger measurements on p-GaN and n-GaN epitaxial layers have been carried out in different modes and different spectrometers. p- and n-GaN epitaxial layers has been measured by AES *as loaded* and than the surfaces has been sputter cleaned by Ar^+ ions. The results are shown in Figs. 3 and 4. Two main conclusions can be drawn from the measurements: (1) there is a reasonable difference in the peak position of p- and n-type GaN for unsputtered and sputtered material, as well, and (2) the Auger peaks shift to higher energetic positions during sputtering for the N KLL Auger peak as well as for the Ga LMM peak. Later measurements confirm, that the peak position difference between sputter cleaned n- and p-type doped GaN-layers is in the 1 to 4 eV range for the Ga LMM peak and for the N KLL peak, respectively. We know [7], that the Fermi level in n-type GaN is approximately 50 meV below the conduction band minimum, the Fermi level in p-type GaN is approximately 250 meV above the valence band maximum. The band gap of the most likely n-conducting surface oxide is about 4.5 eV. According to the band gap the difference in the Auger peak position of n- and p-type GaN should be little smaller than the 3.39 eV. In most of the measurements that is not the case for sputter cleaned GaN. Most measurements show a greater peak position difference than expected, other little smaller ones. Here we can suppose that the sputter induced surface charging depends on the sample structure. It seems that also the sample technology has a distinct influence on the band bending, on the sputtering induced surface charging and therefore on the peak shifts. Figure 5 shows the peak position of different p- and n- conducting GaN samples, *as loaded* as well as on sputter cleaned surfaces. One can see that for all types of the samples, there is a distinct difference between n- and p-type GaN heteroepitaxial layers. In this case, the peak shift from the *as loaded* to the sputter cleaned samples can be described as a result of the removal of surface oxide and contamination layers (iv) as well as the sputtering induced surface charging and resulting band bending (ii).

The detectability of the conduction type has been tested by a line scan measurement over a lateral pn-structure, which was assembled by mounting a p- and n-conducting sample side by side in contact on the sample holder. The SEM micrograph and the results of the peak position measurement over the linescan of the Ga MNN Auger peak is displayed in Fig. 6. A clear peak shift from lower towards higher Auger energies was detectable from the n- to the p-conducting GaN surface. The sample has been sputter cleaned until the absence of oxygen. The amount of the peak shift was approximately 4 eV.

A GaN pn diode for optoelectronic purpose has been prepared by MOCVD. On a SiC substrate and a buffer layer of 450 nm AlGaN an n conducting GaN layer of 450 nm thickness was grown. On the top of that sandwich a Mg doped p conducting GaN layer of 180 nm was epitaxially deposited. An Auger sputter depth profile has been carried out on that sample using Ar^+ ions of 1 keV under 75° with respect to the surface normal. The depth profile is shown in Fig. 7. The depth profile has been carried out until the n conducting GaN was reached and no more peak shifts could be detected. The interface of the pn junction is relatively wide. The contribution of the surface and interface roughness cannot be responsible for that blurring of the interface alone. Surface roughness has been detected by AFM, the FWHM was measured to be 20 nm over an area of $20\mu\text{m} \times 20\mu\text{m}$. Contributions of the space charge region of the pn junction can result in additional broadening of the measured interface width. The same sample has been broken and mounted vertically on an Auger spectrometer sample holder in order to measure a cross section. Point measurements, area measurements and line scans have been carried out. Finally a Scanning Auger mapping was recorded with two special conditions, one providing maximum signal for n-GaN and the second providing maximum signal for p-GaN. The SEM micrograph of the cross section as well as the two Auger maps of n- and p- conducting GaN are shown in Fig. 8 and Fig. 9, respectively. Before recording the Auger maps the

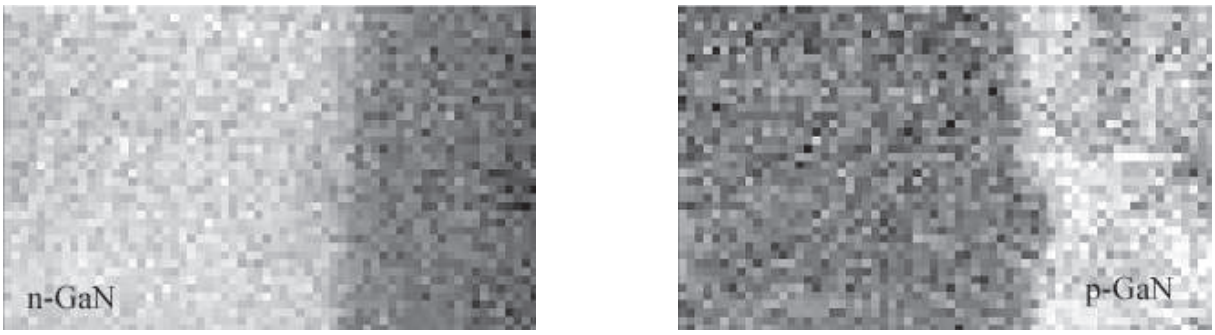

Fig. 9. Auger maps of a) n-conducting GaN and b) p-conducting GaN of the area shown in Fig. 8

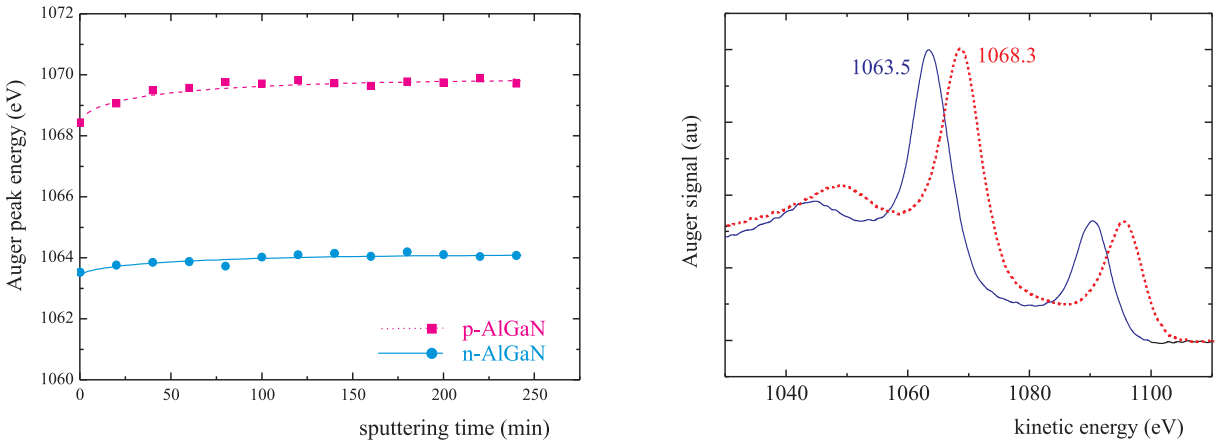

Fig. 10. Auger peak position development of Ga LMM Auger peaks during sputter etching for p- and n-doped $Al_{0.23}Ga_{0.77}N$

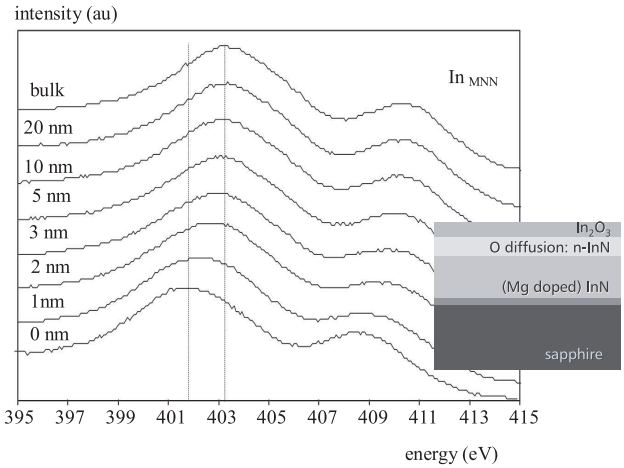

Fig. 11. Auger peak position development of the In MNN Auger peaks during sputter etching through the InN layer sample as indicated in the inset

sample was sputter cleaned in order to remove surface oxide and contaminations on the fractured surface.

The investigations of the polarity of GaN epitaxial layers and its influence on the peak position is published elsewhere [8]. The difference of the Auger peak position from Ga face to N face GaN and therefore the difference of the work function of both polarities could be measured by AES on a lateral polarity sample. The difference was about 0.25 eV with the Ga face GaN having a higher work function.

4.2 AlGaN

Measuring the Auger peak positions of p- and n-doped AlGaN of a constant Al concentration, the results should show the same tendency. We used a AlGaN sample grown by MOCVD of an Al content of about 0.23. Following the predictions of the literature [9] with a bowing coefficient of 0.9 this $Al_{0.23}Ga_{0.77}N$ heteroepitaxial layer should have an energy gap of 4.19 eV. The results of the Auger measurements of the unsputtered n- and p conducting AlGaN samples as well as the Auger peak position development during sputtering are shown in Fig. 10. As supposed, the peak difference from n- to p-type is greater than for pure GaN because of the wider band gap. On the other hand the difference is greater than the estimated band gap of 4.19 eV due to additional band bending factors as sputtering induced charging and the natural surface band bending.

4.3 Indiumnitride

InN has a band gap of approximately only 0.7 eV [10], so the peak shift from n- to p-type InN should be reasonable smaller. All MBE and MOVPE grown undoped InN samples show a heavy n- conduction, especially at the surface [10–13]. On the other hand it is not clear yet, whether Mg doping creates really p-conducting InN layers or only a compensation of the n-conductivity. Measurements indicate, that the surface of Mg doped InN epitaxial layers is n-conducting because of the oxygen incorporation due to the exposure to the atmosphere [11]. We measured a sample with an InN top layer, which was doped with Mg and found a peak shift from the surface to the bulk as displayed in Fig. 11. The three characteristic peak positions of the In MNN peak indicate the three states: (i) indium oxide at the surface with a band gap of much more than 2 eV, (ii) n-conducting InN because of the doping by incorporated oxygen and (iii) p-type or compensated InN in the Mg doped InN layer. The uncertainty of the peak shift due to sputtering induced band bending and the accuracy of the measurements is not sufficient enough to distinguish between p-conducting and compensation within Mg doped InN. But comparing this measurement with those carried out at undoped InN layers, we found, that the Mg doped InN layer is not p-conducting but rather compensated. The results are published in [12]

5 CONCLUSIONS

The Auger peak position measurements have proofed to be a useful method for the detection of the Fermi level position and consequently of the conduction type of group III nitride semiconductor device structures. After first investigations on n- and p-type Si, n- and p-type SiC and different SiC polytypes this method has been successfully applied to GaN, AlGaN and InN structures. It could be shown, that a vertical GaN p-n-junction could be detected by a cross sectional Auger mapping. Peak positions show significant differences between n- and p-type GaN and AlGaN, the difference increases with the width of the band gap. The main advantage of the analytical method AES is the exquisite spatial resolution in combination with the high surface sensitivity. For that reason, AES peak position measurements can be carried out on laterally as well as on vertically micro- and nanostructured samples and layers. The applicability of the Auger peak position measurements has been tested even on small band gap material InN and on lateral polarity GaN structures, where Auger peak shifts down to 0.25 eV can by detected with a high energy resolution electron spectrometer.

Acknowledgement

The work has been supported by Thuringian ministry of education and the Deutsche Forschungsgemeinschaft for the money for the new Microlab 350, by projects of the Thuringian ministry of education (B609-02004), of the Deutsche Forschungsgemeinschaft (AM10571-1), of the Office of Naval Reasearch (Nicop) and by the projects of Scientific Grant Agency of the Ministry of Education of the Slovak Republic (1/1054/04) and Nem/Slov/1/DAAD.

References

[1] VASILYEV, M. G.—KLYACHKO, D. V.—KRIGEL, V. G.—RAZUMOVSKAYA, I. V.: Poverchnost' No. 1 (1985), 97.

[2] KESLER, V. G.—LOGVINSKY, L. M.—PETRENKO, I. P.—SVITASHEV, K. K.: Proc. of the 6th European Conference.

[3] KOSIBA, R.: Augerelektronenspektroskopie und niederenergetischer Ionenbeschuss von Siliziumkarbid, Thesis, TU Ilmenau 2004.

[4] CAI, D.—XU, F.—KANG, J.—GIBART, P.—BEAUMONT, B.: APL 86, 211917 (2005).

[5] HOFMANN, S.: Chapter 4 in Practical Surface Analysis, Vol. 1 — Auger and X-Rray Photoelectron Spectroscopy (D. Briggs and M. P. Seah, eds.), Wiley, Chinchester, 1990.

[6] WU, C. I.—KAHN, A.—TASKAR, N.—DORMAN, D.—GALLAGHER, D.: J. Appl. Phys. **83** No. 8 (1998), 4249–4252.

[7] Elektronenenergie-Verlustspektroskopie an Gruppe-III-Nitriden und Übergangsmetall-Oxiden, Thesis W. Niessner, University Giessen 2002.

[8] NIEBELSCHÜTZ, M.—ECKE, G.—CIMALLA, V.–TONISCH, K.—AMBACHER, O.: J. Appl. Phys. **100** (2006), 074909.

[9] LEE, S. R.—WRIGHT, A. F.—CRAWFORD, M. H.—PETERSEN, G. A.—HAN, J.—BIEFELD, R. M.: Appl. Phys. Let. **74** No. 22 (1999), 3344–3346.

[10] GOLDHAHN, R.—SCHLEY, P.—WINZER, A. T.—GOBSCH, G.—CIMALLA, V.—AMBACHER, O.—RAKEL, M.—COBUT, C.—ESSER, N.—LU, H.—SCHAFF, W. J.: Phys. Stat. Sol. (a) **203** (2006), 42–49.

[11] CIMALLA, V.—NIEBELSCHÜTZ, M.—ECKE, G.—AMBACHER, O.—GOLDHAHN, R.—LU, H.—SCHAFF, W. J.: Phys. Stat. Sol. (c) **3** (2006), 1721–1724.

[12] CIMALLA,V.—NIEBELSCHÜTZ,M.—ECKE,G.—LEBEDEV, V. —AMBACHER,O.—HIMMERLICH,M.—KRISCHOK,S.—SCHAEFER,J. A.— LU,H.—SCHAFF,W.J.: Phys. Stat. Sol. (a) **203** No. 1 (2006), 59.

[13] CIMALLA, V.—ECKE, G.—NIEBELSCHÜTZ, M.—AMBACHER, O.—GOLDHAHN, R.—LU, H.—SCHAFF, W. J.: Phys. Stat. Sol. (c) **7** (2005), 2254–2257.

Received 7 January 2006